In silico CDM model sheds light on force transmission in cell from focal adhesions to nucleus

Jean-Louis Milan, Ian Manifacier, Kevin M. Beussman, Sangyoon J. Han, Nathan J. Sniadecki, Imad About, Patrick Chabrand

Title :

In silico CDM model sheds light on force transmission in cell from focal adhesions to nucleus

Jean-Louis Milan [a,b,n], Ian Manifacier [a,b], Kevin M. Beussman [c], Sangyoon J. Han [c], Nathan J. Sniadecki [c], Imad About [a,b], Patrick Chabrand [a,b]

[a] Aix Marseille Univ, CNRS, ISM, Inst Movement Sci, Marseille, France

[b] APHM, Sainte-Marguerite Hospital, Institute for Locomotion, Department of Orthopaedics and Traumatology, Marseille, France

[c] University of Washington, Seattle, WA, USA

Accepted the 24th of May 2016 and published in Journal of Biomechanics 49 (2016) 2625–2634

http://dx.doi.org/10.1016/j.jbiomech.2016.05.031

***Corresponding author:**

Jean-Louis Milan

Tel.: +33(0)4 91 26 61 45

Fax: +33(0)4 91 41 16 91

E-mail address: jean-louis.milan@univ-amu.fr

Keywords: mechanotransduction; cell mechanics; computational modeling; cell adhesion

Abstract

Cell adhesion is crucial for many types of cell, conditioning differentiation, proliferation and protein synthesis. As a mechanical process, cell adhesion involves forces exerted by the cytoskeleton and transmitted by focal adhesions, forces that constitute signals for specific biological responses. Therefore taking into account cellular mechanotransduction could lead to a better understanding of how, for instance, the shape of adherent stem cells influences their differentiation. To assess the mechanical signals involved in cell adhesion, we computed intracellular forces using the Cytoskeleton Divided Medium model in endothelial cells adherent on microposts. The microposts indicated focal adhesion location and forces, which were then introduced into the model. Then the cytoskeleton and the nucleoskeleton were computed as systems of multiple tensile and compressive interactions in equilibrium with the measured focal adhesion forces. The results indicate that not only the level of adhesion forces but also the shape of the cell has an influence on intracellular tonus and on nucleus strain. The present model for computing mechanotransduction shows promise as a tool for exploring cell mechanobiology.

1. Introduction

Cell adhesion is a mechanobiological process involving cytoskeleton (CSK) dynamics. Moreover, the mechanical aspect of cell adhesion may play an epigenetic role, influencing cell phenotype. For instance there is evidence that the shape and structure reached by stem cells at the end of adhesion affect their differentiation (McBeath 2004, Engler 2006, Kilian 2010; McNamara 2010). Controlling cell adhesion, therefore, is currently one of the main research aims in tissue engineering and biomaterials.

During adhesion, transmembrane complexes such as integrins are able to connect specific proteins in the matrix or those adsorbed on the substrate surface. This leads to creation and maturation of focal adhesions (FAs). Then CSK rearranges, forming stress fibers connecting

FAs, and spatially organizes internal cellular organelles, such as the nucleus. FAs are able to withstand the CSK actin-myosin contraction the cell produces to increase its stiffness and stability (Balaban 2001, Del Rio 2009). They are also the location for the initial mechanotransduction processes, via activation of talin, Rho-A kinase, involved in CSK contraction (Geiger 2009, Wang 2009). CSK tonus has been shown to play an important role in determining cell fate (McBeath 2004, Bhadriraju 2007, Kilian 2010). CSK tonus can be transmitted to the nucleoskeleton (NSK) leading to nuclear deformation (Dahl 2008, Nathan 2011), opening of the membrane ion channel and calcium entry, thereby inducing transcription of specific genes (Itano 2003). Moreover, deformation of the nucleus causes repositioning of chromosomes and so affects gene transcription, as observed in cells whose nucleus is confined by both CSK and substrate micro-grooved topography (McNamara 2012). Understanding mechanotransduction during cell adhesion thus requires taking into account CSK tonus, which appears to be a signal for mechanosensitive complexes from FAs to the nucleus.

Previous work measured the magnitude of force at FAs experimentally (Tan 2003, Fu 2010, Legant 2010, Rape 2011). However, no attempt has been made to measure the magnitude of intracellular forces, in particular the degree of force transmitted to the nucleus. To estimate and understand the internal mechanical state of adherent cells, we developed a numerical model based on tensegrity theory and divided medium mechanics. Tensegrity models take into account the pre-stress of the contractile CSK and provide, in opposition to continuum approach of finite element models, a discrete representation of the filamentous structure of the CSK (Stamenović 1996, Ingber 1997, Ingber 2003, Wendling 2003, McGarry 2004, Maurin 2008). In order to represent CSK rearrangement by (dis)assembling of filaments, we previously developed a tensegrity 2D model based on divided medium mechanics able to introduce evolving connectivity (Milan 2007). This Cytoskeleton Divided Medium (CDM) model was an equilibrated system of multiple tensile and compressive interactions representing CSK

structure. During CDM model deformation, interactions can appear or vanish according to their mechanical properties. This introduces changes in model connectivity and predicts major CSK reorganization. The various CSK filament networks, such as stress fibers, sub-membrane actin cortex, microtubules and intermediate filaments, were included in the model through a biomimetic approach, and their contribution to the overall mechanical behavior of the cell was analyzed. The CDM, extended in 3D, was used to represent cell adhesion on the coated substrate via an iterative process (Milan 2013), and to compute the mechanical state of adherent cells depending on FA spatial distribution. However, precise computation of the intracellular mechanical state depends on knowledge of the full boundary conditions, including both the spatial distribution of the PFAs and the forces they withstand. In the current study, therefore, we investigated adherent cells previously cultured on microposts (Yang 2011), taking micropost deflection as indicating the traction forces exerted by the CSK on FAs. Using these data, we virtually computed a contractile CSK exerting on FAs the same traction forces as those measured experimentally. The computed CSK provided the internal distribution of intracellular tension and, most importantly, the degree of force transmitted to the nucleus. We identified non-linear laws governing interaction between FA forces, intracellular tonus, cell diameter and nucleus strain, and which shed light on intracellular mechanotransduction during cell adhesion.

2. Materials and Methods

The 3D CDM model used here was developed in one of our previous studies (Milan 2013). We extend the previous study by computing the mechanical state of cultured adherent cells, taking into account cellular morphologies and the magnitude of force actually exerted by the cells on their focal adhesions. The present study provides an accurate picture of the real amount of force in the observed cells, as well as of the spatial distribution of forces and their effect on the nucleus.

2.1. Description of the CDM model

The CDM model represented a 15 µm diameter round cell with a 6 µm-diameter nucleus. Cell volume was divided into 12 000 spherical particles of diameters ranging between [0.4; 0.8] µm. Particle centers defined the nodes of the divided medium and of the network of interactions. Nodes were classified by species: *nucleus core*, *nucleus lamina*, *perinuclears*, *cell core*, *cell membrane*, *FAs* (Fig. 1). Interactions between node species were ruled as a relationship between reaction force and gap. Two interaction laws, *Elastic Wire* and *Contact*, were used. Elastic Wire law acted like a virtual pre-strained elastic wire between two nodes: tension was proportional to stretching and became null when the elastic wire slackened. Contact law ruled interactions between the rigid spherical envelopes surrounding the nodes in generating compression force high enough to prevent envelop interpenetration. To reproduce in the CDM model the various components of the CSK and NSK, specific interaction laws were derived from the basic Elastic Wire and Contact laws (Tables 1 and 2). Nuclear lamina was reproduced by high-tensile *LAMIN* interactions between nuclear envelope nodes. Actin filaments were represented in by low-tensile interactions, termed *short F-ACTIN*, creating cortical network between nodes of cell envelop as well as a diffuse network between cell core nodes. Actin filaments that form stress fibers were represented in the model by high-tensile interactions, termed *long F-ACTIN*, connecting focal adhesion nodes to perinuclear nodes and cortex nodes. The dense and unstretched network of intermediate filaments around the nucleus and connected to actin network (Green 1986) were represented by *INTER.FIL* tensile and slackened interactions which connected the long F-ACTIN network to the nuclear LAMIN network. Microtubules, known to bear compression forces in cells (Brangwynne 2006, Kurachi 1995), were represented by *MICROTUBULE* law which was derived from Contact law and generated a compressive force network in the CDM model.

2.2. CSK computation depending on real FA traction forces

Computations of CSK structure and contractility were made on 4 adherent cells provided by Mikael Yang and Christopher Chen, at the time working at the Tissue Microfabrication Laboratory, University of Pennsylvania. They were obtained by culturing in vitro human umbilical vein endothelial cells (HUVECs) in serum on elastomeric micropost substrates (Yang 2011). In this study, microposts are 1.83µm in diameter, 8.3 µm high, and from 4µm-center to center-spaced. For each of these 4 cells, the locations of FAs on microposts were determined experimentally. The forces exerted at these FAs by the CSK were measured as linearly proportional to the deflection of the micropost tips, taking an average stiffness of 7.22nN/µm. These data were imported in the model. First, the CDM was forced to strain iteratively on the substrate until it connected the FA sites of one of the 4 cultured cells (Milan 2013). Since adhesion forces are the signature of the CSK in terms of spatial organization and level of contraction, we sought here to compute, for the 4 cultured cells, the contractile CSK taking FA forces measured experimentally. For a contractile CSK computed via the cell model to be valid, we considered that it should lead to the same signature, i.e that it should exert on the FA nodes the same forces as those reported experimentally. Computing the CSK can be seen as an inverse problem in mechanics. We therefore considered that stress fibers connecting FA would be governed independently. At this stage, for each FA of number i, FA_i, we defined SF_i, a specific law of interaction between perinuclear nodes and FA_i while long F-ACTIN interactions remained activated (Table 1). Iteratively, SF_i stiffness was adjusted and the global equilibrium was computed using LMGC90 code (Dubois 2006) until the cell model exerted on FAs the same traction forces as those measured experimentally. We started by defining all SF_i laws with a rigidity K_i set at 1N/strain. At every following iteration, every K_i was multiplied by the ratio between the force magnitude computed at FA_i node and the experimental force magnitude. This local modification in SF_i rigidity changed not only the forces exerted on FA_i but the whole

network of interactions in the model, and consequently the traction exerted on the other FAs. For this reason, several iterations were required to reach convergence; computations were considered convergent when the relative differences between computed and experimental FA forces were less than 0.1% on average.

In order to monitor intracellular tension, we introduced the index *T,* intracellular tonus, which was computed as the sum of all Elastic Wire interaction forces through the plane located in the middle of the cell and perpendicular to the direction of maximum tension. In the same way, intranuclear tonus $T_{nucleus}$ was defined. To describe the tridimensional deformation of the nucleus, octahedral shear strain $\varepsilon_{nucleus\ shear}$ was computed during deformation of the cell model as a norm of differences in nucleus strain in the 3 directions of space.

3. Results

Conditions of adhesion were observed experimentally in 4 cells cultured in vitro on microposts. Cells are numbered 1 to 4 from smallest to largest. Through interpretation of micropost deviation, FAs were located and traction forces exerted on them were measured as shown in Figures 2 to 5 (a). For instance, FA forces above 1nN are about 2 to 5nN on average depending on the cell, with a maximum of 12 nN. Based on the specific adhesion conditions of these 4 cells, their mechanical states were computed using the CDM model. First, the CDM model spreads via an iterative process until it coincides with the morphology of the 4 adherent cells (Fig. 2 to 5 (b)). Note that in the Cell 3 configuration, the deformation of the model, shown as relative diameter variation, reaches 440 %. During the spreading process, the mechanical state of the model changes and the number of active interactions increases. In the initial state, 50,000 interactions deliver non-null force, while in the Cell 4 configuration, for instance, they have reached more than 90,000 by the end of spreading. Of the 4 morphologies, the spread ones have more tensile interactions (short and long F-ACTIN and INTER.FIL) and less compressive

interactions (MICROTUBULE). While SF interactions reach high forces of about 200-500 pN with a maximum of 1-4nN, the magnitude of other tensile and compressive interactions are only about a few pN, with a maximum of 100pN. Thus the CSK structure was recomputed so as to deliver FA forces equivalent to those measured experimentally (Fig. 2 to 5 (a) & (c)). Table 3 shows the final ranges of stress fiber stiffness K_i for the 4 cell configurations: minimum and maximum values can differ by 3 or 4 orders of magnitude. Final values of Ki are on average 20-70 times greater than their initial values, depending on the cell configuration. Depending on the cell configuration, between 28 and 40 iterations are required to converge and to deliver a contractile CSK whose error on FA forces is less than 0.1% on average (Fig. 6). With very few FAs located more towards the center of the cell, error can reach a maximum of 40%. Additional iterations seem to have no effect on convergence. Figure 6 shows clearly how the iterative adjustment of CSK contractility using the present CDM model yields more accurate results than the old 2013 version of the model (iteration 1). By taking into account the specific adhesion conditions of the cell and adjusting local CSK contractility, this error was greatly reduced, from 80% to close to zero.

With an initial intracellular tonus of 3.5 nN, the cell model reached a tonus 46, 34, 20 and 43 times higher in Cells 1 to 4, respectively (Table 4).

The nucleus deformed, first due to the flattening of the whole cell medium as it spread on the plane substrate (Figures 2 to 5 (d)). Secondly, the nucleus stretched, as did the whole cell model. The nucleus is connected to the CSK via INTER.FILs. Initially loose, the INTER.FILs tighten as traction increases in the F-ACTIN network, becoming active bonds between the nucleus and the F-ACTIN network. The model predicts highest nucleus deformation in Cell 3. The computation of $\varepsilon_{nucleus\ shear}$ shows that the nucleus is more strained in more deformed cells (Table 4), the highest deformation being found in Cell 3.

The more the cell model is deformed, the more intracellular tonus is conveyed to the nucleus.

The sum of intracellular force magnitudes transmitted to the nucleus reaches 28, 41, 45 and 35nN in Cells 1 to 4 respectively. For instance in Cell 3, whose diameter is greater than that of the other cells although it has the lowest tonus, the nucleus is subjected to maximum intracellular forces. Intranuclear tonus reaches 0.35, 0.64, 0.85 and 0.44 for cells 1 to 4, respectively. As a consequence, the nucleus structure deforms: the membrane, for instance, deforms on average about 13, 17, 19 and 15 % in Cells 1 to 4, respectively.

As expected, in the CDM model, intracellular tonus appears to be only related to adhesion forces, being equivalent to 40% of the total sum of adhesion force magnitudes (Figure 7). Unexpectedly, nucleus deformation appears more dependent on cell diameter deformation (Figure 8) than on intracellular tension. Indeed the proportion of internal tension that is conveyed to the nucleus does not evolve purely with intracellular tonus, but also with cell diameter. In the 4 cells tested, tension transmitted to nucleus, $T_{to\ nucleus}$, appears to evolve according to the following relation:

$$T_{to\ nucleus} = T^{1.16}.D^{0.92}.AR^{1.85} \qquad (5)$$

where AR is the aspect ratio of the cell top view: 1 if the cell spread area is circular, 0 if it is infinitely elongated. Although it would require a statistical approach to be taken to more adherent cells in order to propose a general relationship, these findings indicate that the more the cell spreads, the more tension is directly conveyed to the nucleus via the intermediate filament network. Moreover, the more the cell spreads on a plane substrate, the more the cell flattens and the more the nucleus is deformed. Overall deformation of the nucleus may thus represent a mechanical signal during cell adhesion. Local deformation of the nucleus membrane, which is about 10-20% on average with a maximum of 100%, may also induce the cation channel opening involved in specific gene transcription.

Discussion

Cell adhesion is a mechanobiological process involving generation of tensile forces by the CSK, focal adhesion reinforcement and potential nucleus strain. These are potential mechanical signals for a specific biological response to occur. Here, we combined novel in vitro methods based on deformable micropost substrates with an original computational approach to evaluate the intracellular forces involved in cell adhesion. Adhesion conditions of 4 cells were measured experimentally in terms of location of FA and force magnitude. Being based on these experimental data, the computation conducted on our CSK Divided-Medium (CDM) model proposed a valid CSK contractile structure and allowed us to chart the intracellular forces in adherent cells. Since it identifies the mechanical forces transmitted by the CSK from the focal adhesions to the deformable nucleus, the CDM model appears able to represent the direct mechanotransduction involved in cell adhesion. This multi-interaction model can represent the quantity of polymerized and reticulated filaments of CSK and the tensile and compressive forces they exert individually. For instance, in Cell 3, the computed CSK was composed of 40 000 1μm-actin filaments in a diffuse network, 12 000 10μm-actin filament forming long stress fibers, 7000 1μm-microtubules forming long chains of compression while 1200 elastic filaments composed the nucleus lamina, all bearing individually forces of 1-10 pN in average. Thanks to the concept of variable mechanical interaction among a discrete number of nodes, the CDM model appears to be able to represent the interconnected filaments that rearrange and compose the various substructures of the CSK and NSK. Thus, the CDM model is a useful alternative to the classic tensegrity model, which has the limitation of fixed connectivity, or the finite element model, which is unable to represent the discrete and changing structure of the cytoskeleton. In addition, as opposed to the previous version of the CDM model in Milan et al. (2013), the present improved model is able to accurately compute the mechanical state of the cell in terms of CSK architecture and pre-stress directly related to the adhesion conditions of

FA location and force (Milan 2013).

The previous version discriminated roughly in cultured cells the influence of adherent shape on intracellular tension, without considering real FA forces and so without real boundary conditions of cells. The model could not, therefore, guarantee that the resulting internal tension was fully consistent with the real mechanical state of the observed cells. Contrastingly, in the present study we computed the contractility of the CSK in such a way that the resulting traction on each FA matched the force magnitude measured experimentally by deflection of the corresponding micropost to which the cell was attached. By incorporating this cell-dependent process, the present model offers the advantage of being able to compute in real cells the actual intracellular forces transiting via the CSK.

This work shows that intracellular tonus may not be correlated only to cell spread area or diameter. For instance, Cell 1, which has the smallest diameter, possesses the highest tonus, while Cell 3 is an example of the opposite, with the largest diameter and the lowest tonus. McBeath et al. (2004) showed that the shape alone can lead to hMSC commitment involving CSK tension (McBeath 2004). The present study shows the positive effect of wide cell spreading on transmitting intracellular tonus to the nucleus via the stretching of the intermediate filament network. The nucleus strain computed is in the same range as that observed experimentally to induce changes in gene expression and cell differentiation (Itano 2003, Dahl 2008, Nathan 2011). Thus, by analyzing the relations between nucleus shape and CSK tonus, our study quantifies the first steps of direct mechanotransduction involved in the cell adhesion process.

4. Conclusion

The present study proposed an estimation of mechanical signals involved during cell adhesion combining in vitro experiments and computational mechanics. Cells were cultured on microposts to measure forces they exerted on focal adhesions. Starting from the experimental adhesion conditions of various cells, a computational model based on a multi-interaction system yielded the internal mechanical state of the cell in terms of cytoskeleton organization, cell tonus and nucleus strain. This indicated that intracellular tonus was not transmitted directly and linearly to the nucleus. Tensile stimulation of the nucleus by the cytoskeleton during adhesion only occurred in highly spread cell morphologies, which in the case of stem cells is known to promote commitment into osteoblasts or fibroblasts. The present model should contribute to a better understanding of mechanotransduction during adhesion involving cell shape, focal adhesion forces, nucleus strain and biological cell activity.

5. Acknowledgements

We acknowledge Michael Yang and Christopher Chen for providing accurate experimental data of cell adhesion forces. The authors have declared that no competing interest exists.

6. References

Balaban NQ, Schwarz US, Riveline D, Goichberg P, Tzur G, Sabanay I, Mahalu D, Safran S, Bershadsky A, Addadi L, Geiger B (2001) Force and focal adhesion assembly: a close relationship studied using elastic micropatterned substrates. Nat Cell Biol 3:466-472

Bhadriraju K, Yang M, Alom Ruiz S, Pirone D, Tan J, Chen CS (2007).Activation of ROCK by RhoA is regulated by cell adhesion, shape, and cytoskeletal tension. Exp. Cell Res 313:3616-3623

Brangwynne, C.P. et al. Microtubules can bear enhanced compressive loads in living cells because of lateral reinforcement. J. Cell Biol.173, 733-741 (2006).

Dahl KN, Ribeiro AJS, Lammerding J (2008) Nuclear shape, mechanics, and mechanotransduction. Circ. Res 102:1307-1318.

Deguchi S, Ohashi T, Sato M (2006) Tensile properties of single stress fibers isolated from cultured vascular smooth muscle cells. J Biomech 39:2603-2610.

Del Rio A, Perez-Jimenez R, Liu R, Roca-Cusachs P, Fernandez JM, Sheetz MP (2009) Stretching single talin rod molecules activates vinculin binding. Science 323:638-641.

Dubois, F. & Jean, M. The non smooth contact dynamic method: recent LMGC90 software developments and application. *Lecture Notes in Applied and Computational Mechanics* **27**, 375–378 (2006).

Engler AJ, Sen S, Sweeney HL, Discher DE (2006). Matrix elasticity directs stem cell lineage specification. Cell 126:677-689.

Fu J, Wang YK, Yang MT, Desai RA, Yu X, Liu Z, Chen CS (2010) Mechanical regulation of cell function with geometrically modulated elastomeric substrates. Nat Methods 7:733-736.

Geiger B, Spatz JP, Bershadsky AD (2009) Environmental sensing through focal adhesions. Nat. Rev. Mol. Cell Biol. 10:21-33.

Green, K.J., Talian, J.C. & Goldman, R.D. Relationship between intermediate filaments and microfilaments in cultured fibroblasts: evidence for common foci during cell spreading. *Cell Motil. Cytoskeleton***6**, 406-418 (1986).

Ingber DE (1997) Tensegrity: the architectural basis of cellular mechanotransduction. Annu. Rev. Physiol 59:575-599.

Ingber DE (2003) Tensegrity I. Cell structure and hierarchical systems biology. J. Cell. Sci 116:1157-1173.

Itano N, Okamoto S, Zhang D, Lipton SA, Ruoslahti E (2003) Cell spreading controls endoplasmic and nuclear calcium: a physical gene regulation pathway from the cell surface

to the nucleus. Proc. Natl. Acad. Sci. U.S.A 100:5181-5186.

Kilian KA, Bugarija B, Lahn BT, Mrksich M. (2010) Geometric cues for directing the differentiation of mesenchymal stem cells. Proc. Natl. Acad. Sci. U.S.A 107:4872-4877.

Kurachi, M., Hoshi, M. & Tashiro, H. Buckling of a single microtubule by optical trapping forces: direct measurement of microtubule rigidity. Cell Motil. Cytoskeleton30, 221-228 (1995).

Legant WR, Miller JS, Blakely BL, Cohen DM, Genin GM, Chen CS (2010) Measurement of mechanical tractions exerted by cells in three-dimensional matrices. Nat. Methods 7:969-971.

Maurin B, Cañadas P, Baudriller H, Montcourrier P, Bettache N (2008) Mechanical model of cytoskeleton structuration during cell adhesion and spreading. J Biomech 41:2036-2041.

McBeath R, Pirone DM, Nelson CM, Bhadriraju K, Chen CS (2004) Cell shape, cytoskeletal tension, and RhoA regulate stem cell lineage commitment. Dev. Cell 6:483-495.

McGarry JG, Prendergast PJ (2004) A three-dimensional finite element model of an adherent eukaryotic cell. Eur Cell Mater 7:27-33.

McNamara LE, McMurray RJ, Biggs MJP, Kantawong F, Oreffo ROC, Dalby MJ (2010) Nanotopographical control of stem cell differentiation. J Tissue Eng 120623

McNamara LE, Burchmore R, Riehle MO, Herzyk P, Biggs MJP, Wilkinson CDW, Curtis ASG, Dalby MJ (2012) The role of microtopography in cellular mechanotransduction. Biomaterials

33:2835-2847

Milan JL, Wendling-Mansuy S, Jean M, Chabrand P (2007) Divided medium-based model for analyzing the dynamic reorganization of the cytoskeleton during cell deformation. Biomech Model Mechanobiol 6:373-390.

Milan JL, Lavenus S, Pilet P, Louarn G, Wendling S, Heymann D, Layrolle P, Chabrand P

(2013) Computational model combined with in vitro experiments to analyze mechanotransduction during mesenchymal stem cell adhesion. European Cells and Materials Journal 25:97-113

Nathan AS, Baker BM, Nerurkar NL, Mauck RL (2011) Mechano-topographic modulation of stem cell nuclear shape on nanofibrous scaffolds. Acta Biomater 7:57-66.

Rasband, W.S., ImageJ, U. S. National Institutes of Health, Bethesda, Maryland, USA, http://imagej.nih.gov/ij/, 1997-2014.

Rape AD, Guo WH, Wang YL -2011) The regulation of traction force in relation to cell shape and focal adhesions. Biomaterials 32:2043-2051.

Stamenović D, Fredberg JJ, Wang N, Butler JP, Ingber DE (1996) A microstructural approach to cytoskeletal mechanics based on tensegrity. J. Theor. Biol 181:125-136.

Tan JL, Tien J, Pirone DM, Gray DS, Bhadriraju K, Chen CS (2003) Cells lying on a bed of microneedles: an approach to isolate mechanical force. Proc Natl Acad Sci USA 100:1484-1489.

Wang N, Tytell JD, Ingber DE (2009) Mechanotransduction at a distance: mechanically coupling the extracellular matrix with the nucleus. Nat. Rev. Mol. Cell Biol 10:75-82.

Wendling S, Cañadas P, Chabrand P (2003) Toward a generalised tensegrity model describing the mechanical behaviour of the cytoskeleton structure. Comput Methods Biomech Biomed Engin 6:45-52.

Yang MT, Reich DH, Chen CS (2011) Measurement and Analysis of Traction Force Dynamics in Response to Vasoactive Agonists. Integrative Biology. 3(6): 663-674.

Yang MT, Fu J, Wang YK, Desai RA, Chen CS (2011). Assaying stem cell mechanobiology on microfabricated elastomeric substrates with geometrically modulated rigidity. Nature Protocols. 6(2):187-213

Figure and table legends

Figure 1: Structure of the CDM model at round state (diameter = 15µm). Cell geometry was represented by a divided medium with nodes composed of different species: a) nucleus core (pink), b) nucleus membrane (yellow) and perinuclear nodes (blue) c) cell core nodes (orange) d) cell membrane (red).

Figure 2: Cell 1. Model results vs in vitro measurements. a) Spatial distribution of FAs and adhesion force magnitudes measured experimentally. b) Spreading of CDM model until it matched experimental adhesion conditions ; top and side view. c) Adhesion force magnitudes computed after iterative CSK computation. d) Strained nucleus in yellow ; top and side view. Scales are in µm

Figure 3: Cell 2. Model results vs in vitro measurements. See Fig. 2 for description of a) to d).

Figure 4: Cell 3. Model results vs in vitro measurements. See Fig. 2 for description of a) to d).

Figure 5: Cell 4. Model results vs in vitro measurements. See Fig. 2 for description of a) to d).

Figure 6: Convergence of CSK computation in the 4 in vitro cells. Evolution of error between computed and measured FA forces over iterations.

Figure 7: Comparison between intracellular tonus computed in the 4 adherent cells and their total force of adhesion and diameter.

Figure 8: Evolution of nucleus strain depending on cell strain and cell tonus.

Table 1: Table of interactions between the various node species represented in the CDM model, the cytoskeleton substructures and the nucleoskeleton. For every law of interaction, the value of the maximum gap between nodes above which interaction vanishes is reported in µm in brackets. The interaction law SFi between Perinuclears and FA_i was only activated in the CSK computation described in Methods 2.3.

Table 2: Interaction law parameters.

Table 3: Final ranges of stress fiber stiffness K_i in the CDM model for the 4 cell configurations.

Table 4: Experimental measurements and computational estimations of morphological and mechanical properties in the 4 cells using the CDM model. D and d, max and min cell diameters ; $\Delta D/D0$, relative diameter variation of the model from initial spherical state to cell shape. D_n and d_n, max and min nucleus diameters.

Figure 1
Click here to download high resolution image

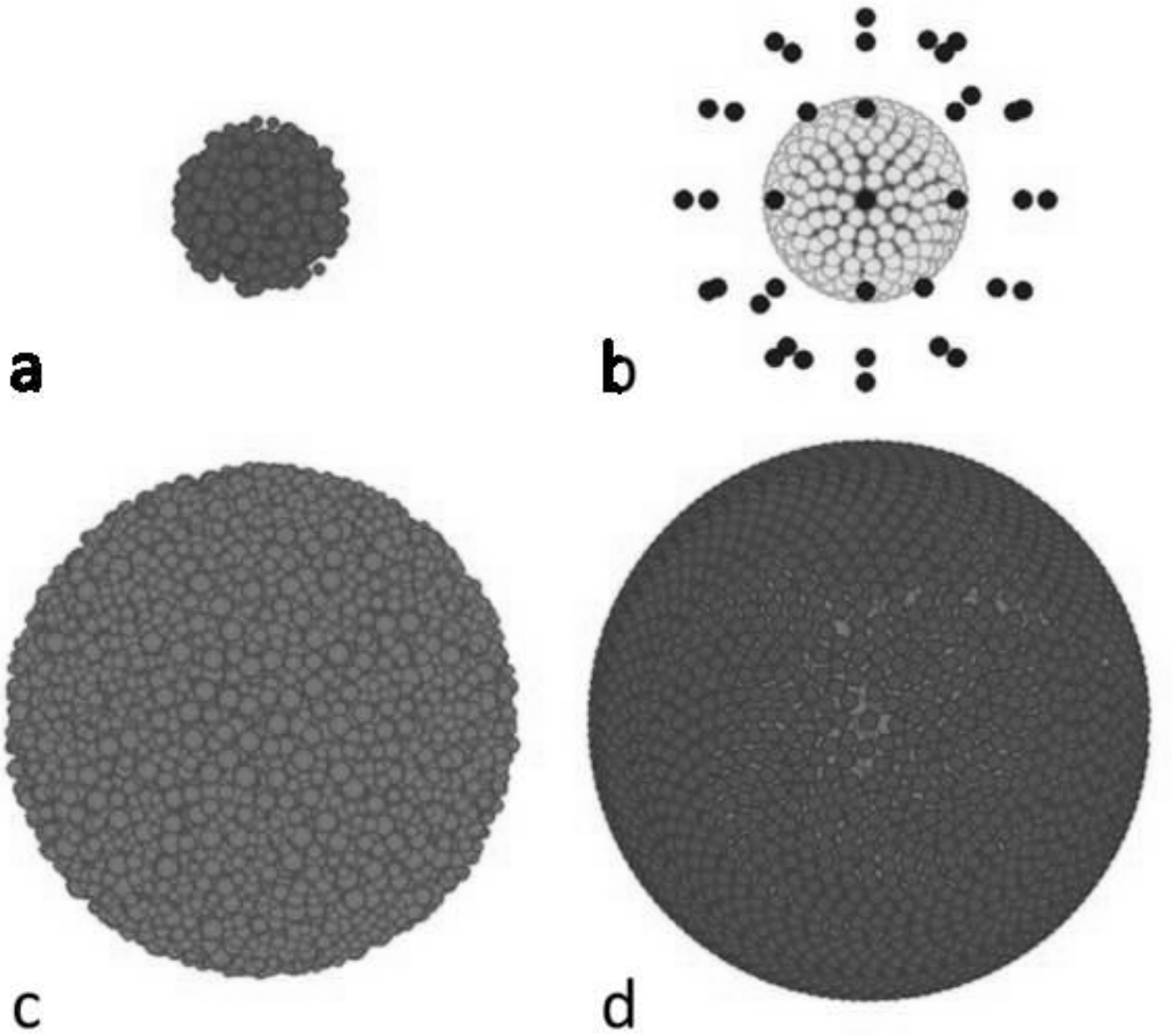

Figure 2
Click here to download high resolution image

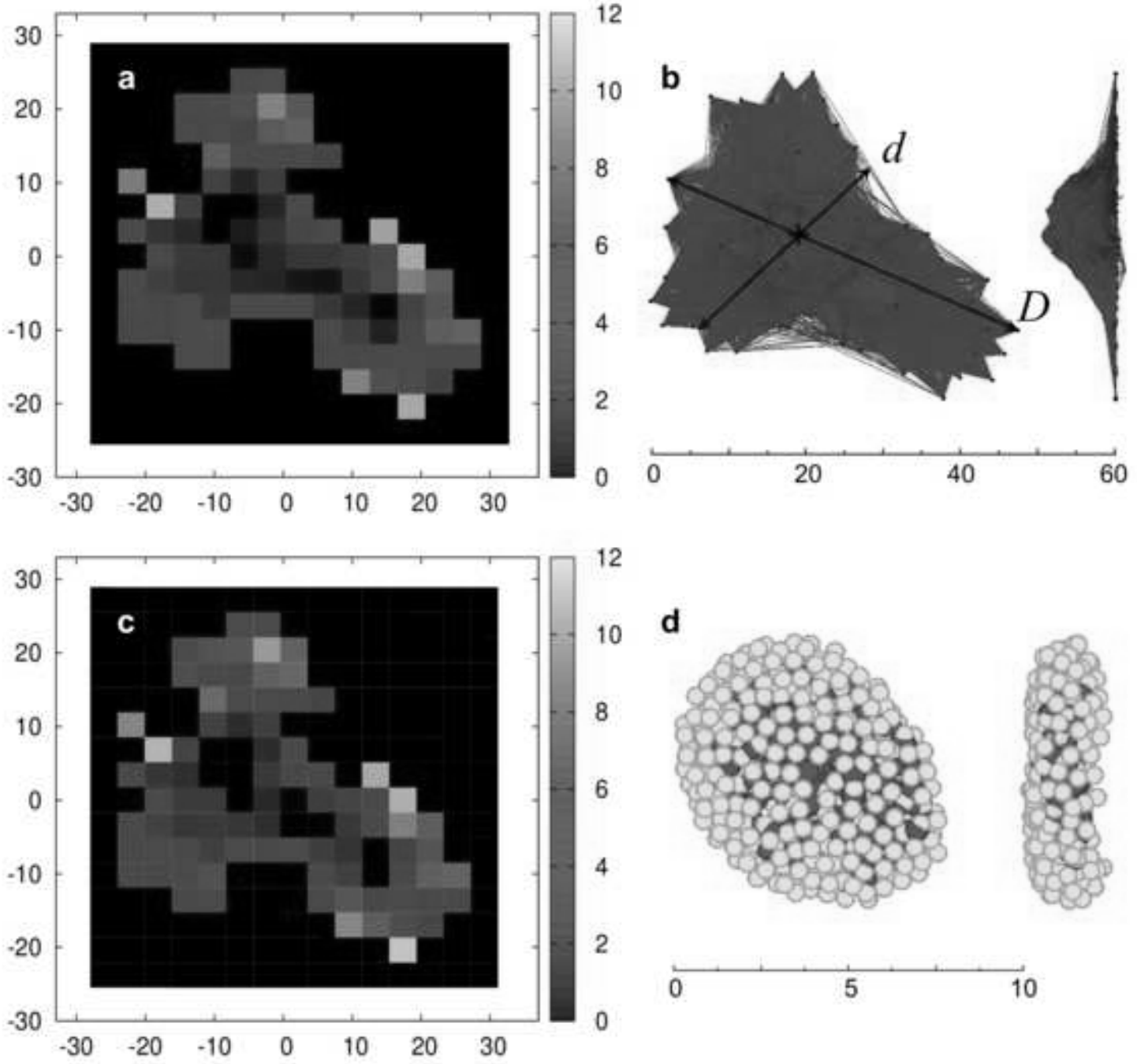

Figure 3
Click here to download high resolution image

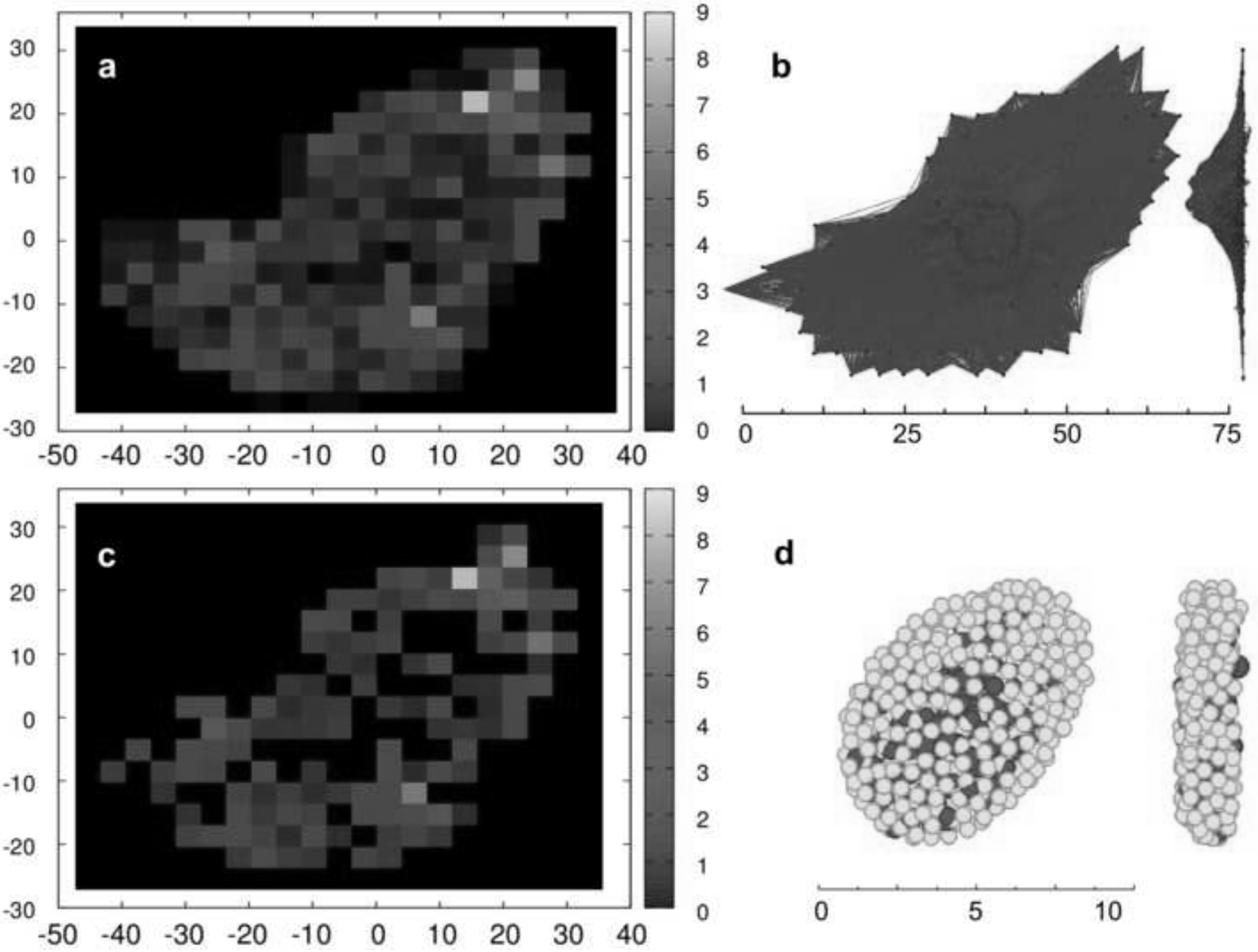

Figure 4
Click here to download high resolution image

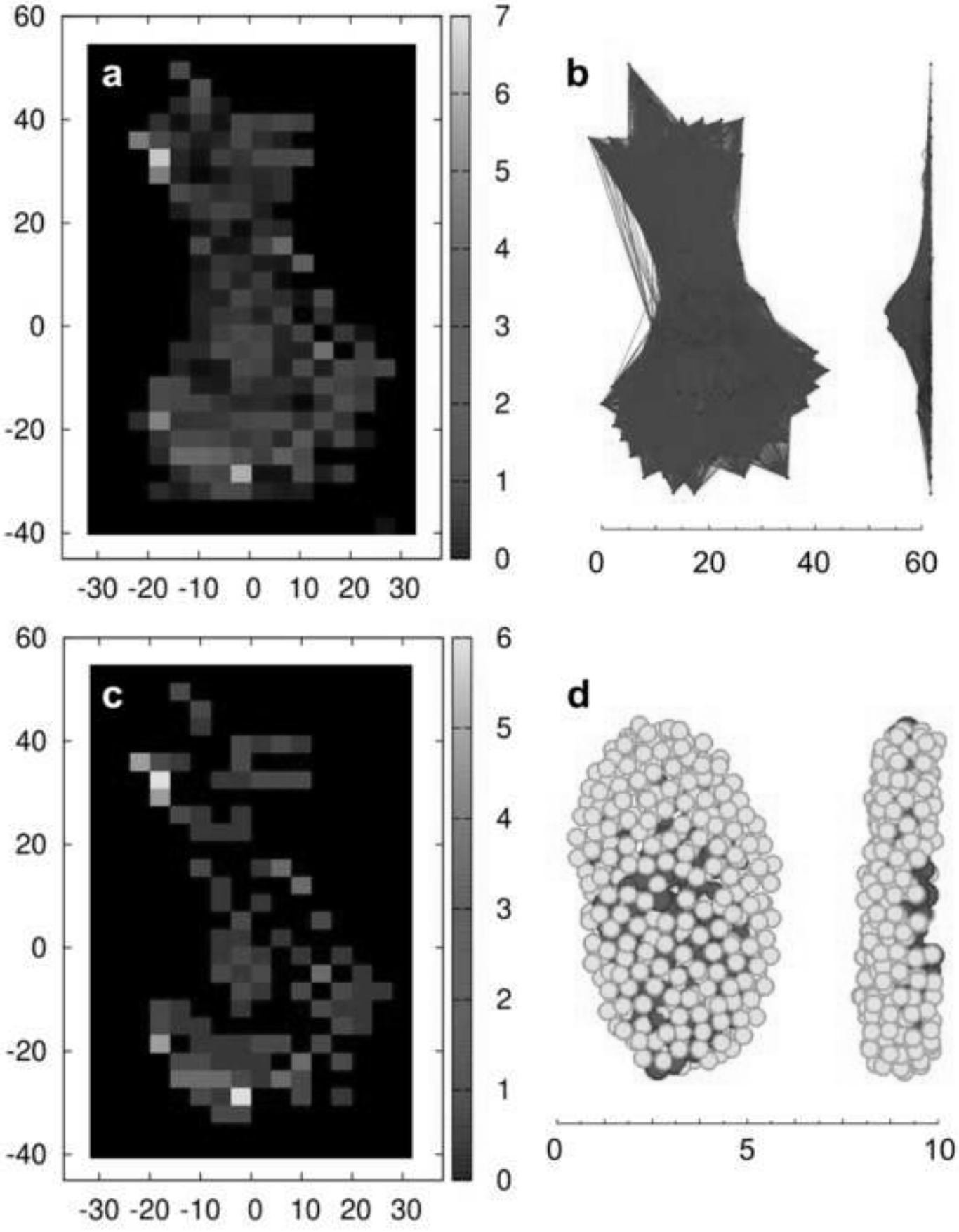

Figure 5
Click here to download high resolution image

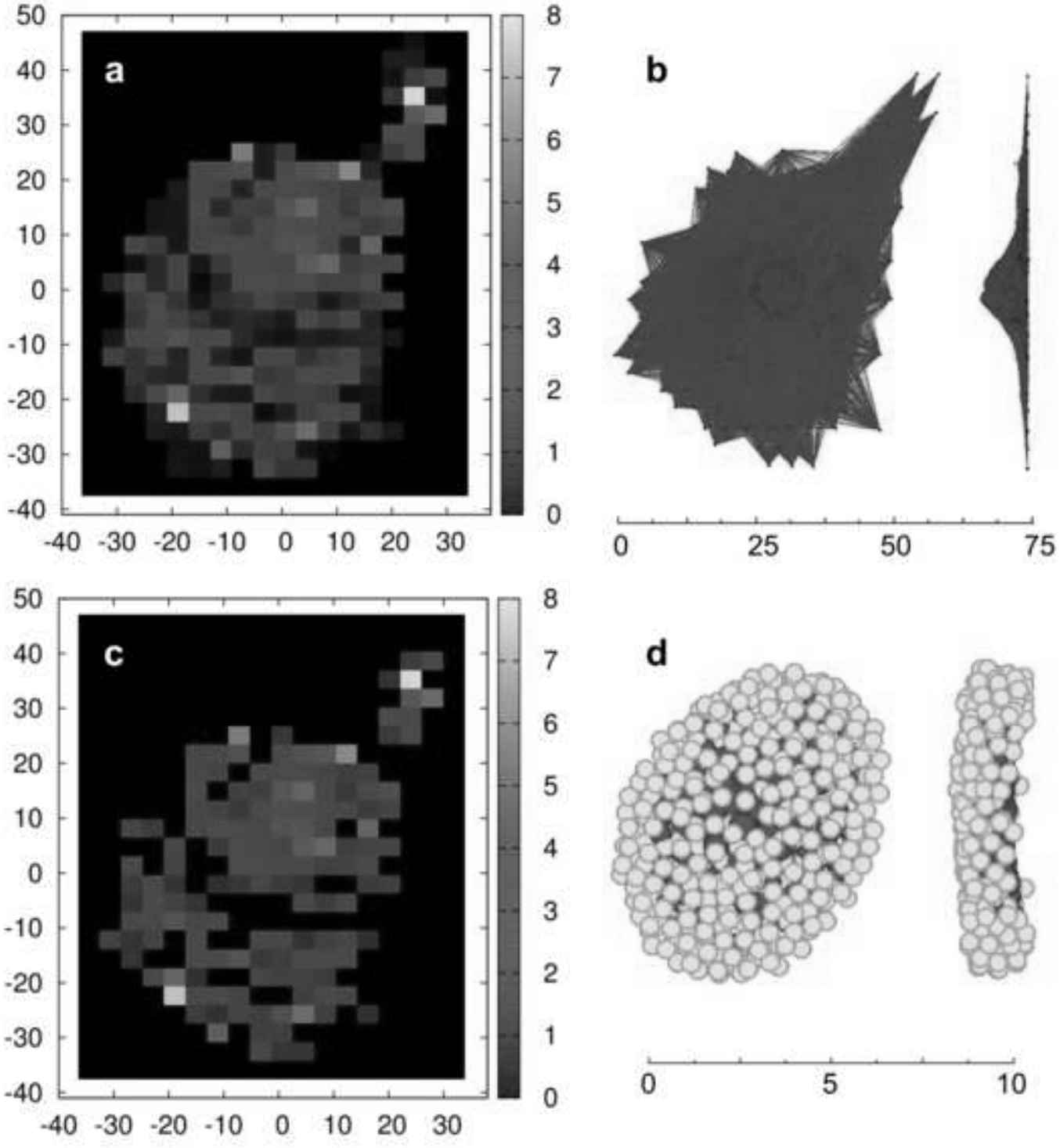

Figure 6
Click here to download high resolution image

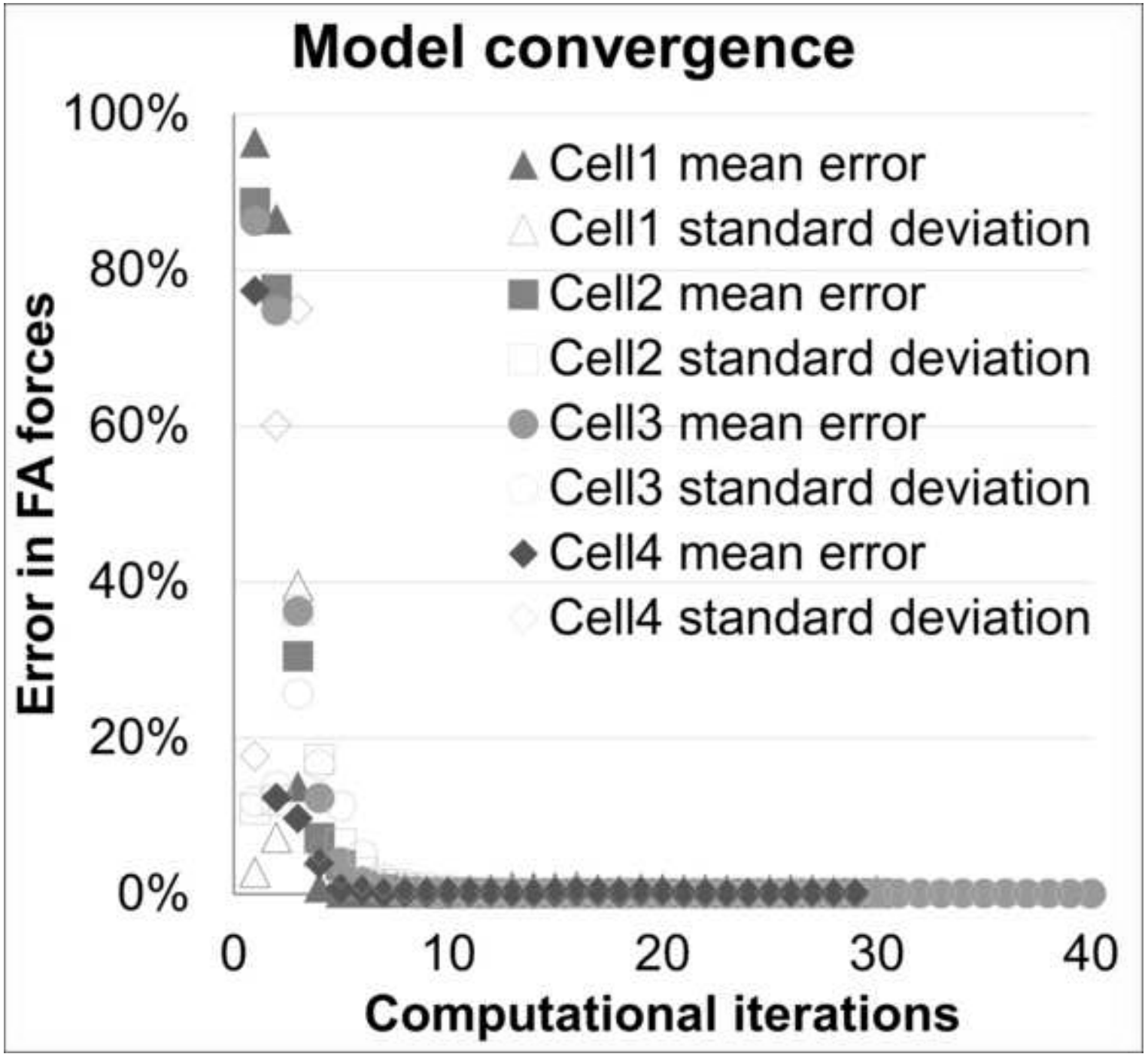

Figure 7
Click here to download high resolution image

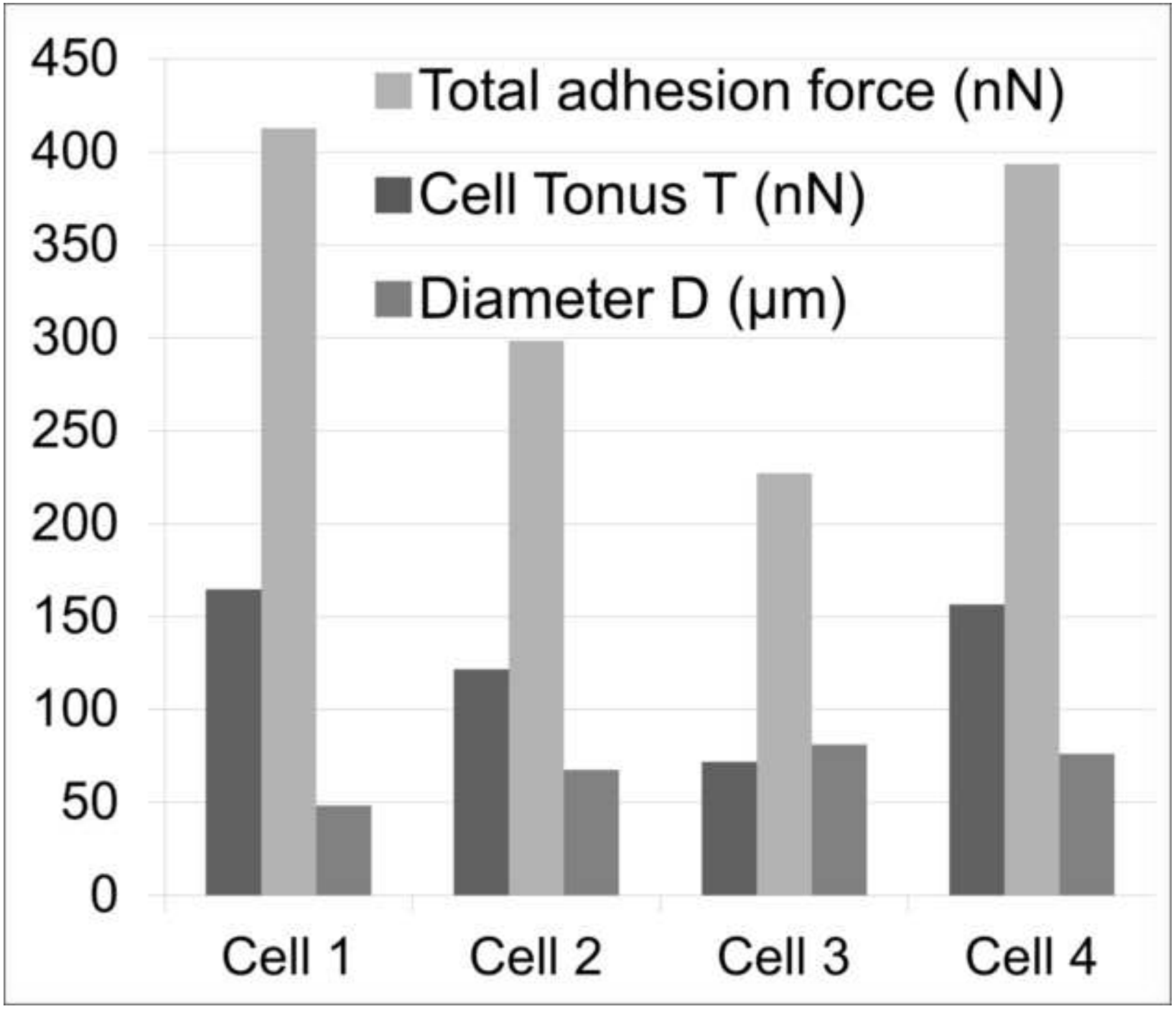

Figure 8
Click here to download high resolution image

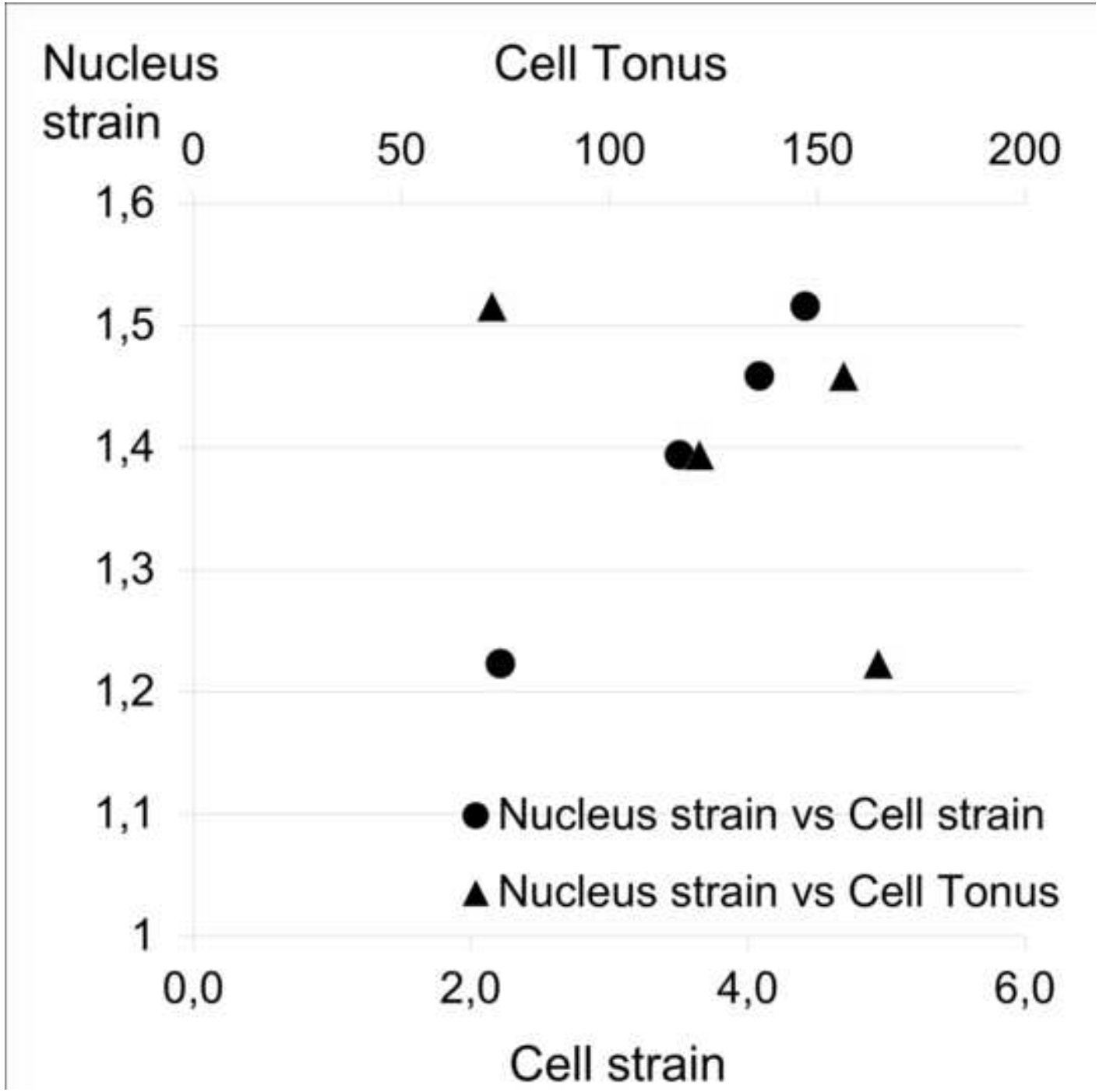

Table 1
Click here to download high resolution image

Nodes	Nucleus core	Nucleus lamina	Perinuclears	Cell core	Cell membrane	FAs
Nucleus core	INTRA-NSK CONTACT	INTRA-NSK CONTACT	CONTACT	CONTACT	CONTACT	CONTACT
Nucleus lamina		LAMIN CONTACT	INTER.FIL CONTACT	CONTACT	CONTACT	CONTACT
Perinuclears			INTER.FIL CONTACT	short F-ACTIN CONTACT	INTER.FIL CONTACT	long F-ACTIN CONTACT SF_i
Cell core				short F-ACTIN MICROTUBULE	short F-ACTIN CONTACT	short F-ACTIN CONTACT
Cell membrane					short F-ACTIN	long F-ACTIN CONTACT
FAs						CONTACT short F-ACTIN
Substrate	CONTACT	CONTACT	CONTACT	CONTACT	CONTACT	CONTACT

Table 2
Click here to download high resolution image

Elastic Wire laws	**Rigidity K (nN/strain)**	**Prestrain τ**
short F-ACTIN (Actin filaments)	3×10^{-4}	1×10^{-3}
long F-ACTIN (Actin fil. in stress fibers)	1×10^{-2}	0.2 [24]
SF_i (stress fibers connecting FA_i)	To be computed	0.2 [24]
INTER.FIL (Intermediate filaments)	2×10^{-2}	-0.1
LAMIN (Nuclear lamina)	4×10^{-2}	0
INTRA-NSK (Intranuclear filaments)	2×10^{-2}	0
Contact laws	**Cohesion c (nN)**	**Rigidity S (nN/strain)**
CONTACT	0	/
MICROTUBULE (Microtubules)	0	1

Table 3
Click here to download high resolution image

K_i (nN/strain)	Cell 1	Cell 2	Cell 3	Cell 4
Min	0.08	0.01	0.01	0.01
Max	5.05	1.43	1.58	23.70
Mean	0.63	0.20	0.17	0.48
Std. deviation	0.09	0.23	0.08	16.75

Table 4
Click here to download high resolution image

Cells		1	2	3	4
In vitro cell measurements					
Spread area (μm²)		960	1809	1855	2183
Diameter (μm)		48	68	81	76
FA number		84	91	118	144
Total traction on FA (nN)		413	299	227	394
Mean traction on FA (nN)		4.9	3.3	1.9	2.7
Computation results on cell mechanics					
Cell strain ($\Delta D/D_0$)		2.2	3.5	4.4	4.1
Cell strain (D/d)		3.2	4.5	5.4	5.1
T (nN)		165	122	72	156
$T / T_{initial}$		46	34	20	43
T / Total FA traction		0.40	0.41	0.32	0.40
Computation results on nucleus mechanics					
Diameter (μm)		8.8	9.7	10.2	9.8
Strain :	$\Delta D_n/D_{n0}$	0.47	0.62	0.70	0.63
	D_n/d_n	1.47	1.62	1.70	1.63
	ε_x	0.31	0.42	0.05	0.28
	ε_y	0.32	0.36	0.69	0.56
	ε_z	-0.55	-0.59	-0.54	-0.58
	$\varepsilon_{nucleus\ shear}$	1.22	1.39	1.52	1.46
$T_{nucleus}$ (nN)		0.35	0.64	0.85	0.44
Membrane strain		0,13	0,17	0,19	0,15

***Conflict of Interest Statement**

The authors have declared that no competing interest exists in the present study '**Model of contractile cytoskeleton to analyze mechanotransduction in adherent cells'**

Jean-Louis Milan, Patrick Chabrand

Aix-Marseille Université, CNRS, ISM UMR 7287, Marseille France